Electronic Supplementary Material (ESI) for Catalysis Science & Technology.
This journal is © The Royal Society of Chemistry 2023

Electronic Supporting Information

MOF-derived $Fe_2O_3/MoSe_2$ Heterostructure for Promoted Electrocatalytic Nitrogen Fixation

Liming Huang [a, b, ‡], Leiming Tao [b, ‡, *], Kui Pang [bc], Shuying He [b], GuanHua Zhu [b], LinHai Duan [b], Chenglin Wen [b], Changlin Yu [b], Hongbing Ji [a, *]

[a] *School of Chemistry and Chemical Engineering, Guangxi University, Nanning, 530003, China.*

[b] *Guangdong Provincial Key Laboratory of Petrochemical Equipment Fault Diagnosis, School of Science, Guangdong University of Petrochemical Technology, Maoming, Guangdong, 525000, China.*

[c] *Engineering Research Center for Nanomaterials, Henan University, Henan, 475001, China*

[*] Corresponding author.

E-mail address： leimingtao@foxmail.com, jihb@mail.sysu.edu.cn

‡ Liming Huang and Leiming Tao contributed equally to this work.

Experimental section

Materials

Sodium Molybdate Dihydrate ($Na_2Mo_4 \cdot 2H_2O$), Ferric Chloride Hexahydrate ($FeCl_3 \cdot 6H_2O$), Sodium Borohydride ($NaBH_4$), Ammonium Chloride (NH_4Cl), Sodium Hydroxide (NaOH), Sodium Nitroferricyanide ($C_5FeN_6Na_2O \cdot 2H_2O$) and Nafion (5 wt%) were purchased from Shanghai Macklin Biochemical Co. Ltd (China). Terephthalic acid ($C_8H_6O_4$), selenium powder (Se), dimethylformamide (DMF), sodium hypochlorite solution (NaClO), sodium sulfate (Na_2SO_4) and sodium salicylate ($C_7H_6O_3Na$), sodium citrate ($C_6H_5Na_3O_7 \cdot 2H_2O$), ethanol ($C_2H_5OH$) and sulfuric acid ($H_2SO_4$) were purchased from Shanghai Aladdin Biochemical Technology Co. Ltd. (China). All chemicals used were of analytical reagent grade and were used as received.

Characterization

The XRD patterns of samples were recorded on D/Max 2500PC diffractometer at a scan rate of 6º min^{-1} from 10º to 80º. The morphologies and nanostructures of all products were characterized by the SEM (JEOL JSM-6510LV) at 15 kV, TEM (JEOL JEM-2100F) at 200 kV and high-angle annular dark-field transmission electron microscopy (HAADF-STEM, JEM-ARM200F) at 200 kV. XPS measurements were conducted with a Thermo ESCALAB 250XI XPS spectrometer. The absorbance data of the spectrophotometer were collected by the Agilent CARY 60 spectrophotometer. The ion chromatography data were collected on Shine CIC-D100 plus using the dual temperature heater, injection valve,

conductivity detector, AERS 500 Anions suppressor. ^{1}H NMR spectra were collected on a superconducting-magnet NMR spectrometer (Bruker Advance III HD 600 MHz). Electrochemical NRR measurements were performed over electrochemical working station (CHI 760E, Shanghai CH Instruments Co., China)

Preparation of Fe_2O_3

Fe metal-organic framework (Fe-MOF)-derived Fe_2O_3 materials were synthesized using the method of Wei et al[1]. First, 1.8245 g $FeCl_3 \cdot 6H_2O$ and 0.7476 g $C_8H_6O_4$ have dissolved in 40 mL DMF solution under vigorous magnetic stirring for 1 h. The resulting homogeneous solution was then transferred to a 100 mL Teflon-lined stainless steel autoclave and heated at 120 °C for 15 h. The solid orange Fe-MOF obtained after cooling the reaction mixture to room temperature was washed three times with distilled water and centrifuged to dry overnight. Then, the obtained Fe-MOF was placed in a ceramic crucible and heated to 350 °C in the air at a heating rate of 2 °C min^{-1} in a tube furnace for 2 h to prepare Fe-MOF-derived Fe_2O_3 nanoparticles.

Preparation of original $MoSe_2$

Thereafter, 0.304 g $NaBH_4$, 0.316 g Se, and 0.484 g Na_2MoO_4 were mixed together and dissolved in 60 mL of distilled water with vigorous magnetic stirring for 20 min to obtain a homogeneous solution. The solution was then transferred to a 100 mL Teflon-lined stainless steel autoclave heated to 200 °C and held at the target temperature for 20 h. After natural cooling, the black precipitate was collected by centrifugation, washed several times with deionized water and absolute ethanol, and dried under vacuum at 60 °C.

Preparation of $Fe_2O_3/MoSe_2$ composites

The prepared Fe_2O_3 nanoparticles (0.1g, 0.2g, 0.3g or 0.4g) were added to the above solution. The solution was then transferred to a 100 mL Teflon-lined stainless steel autoclave and heated at 200 °C for 20 h. After the above solution was naturally cooled to room temperature, the obtained $Fe_2O_3/MoSe_2$ composites were collected by centrifugation and then washed with distilled water and ethanol several times. Finally, the obtained black solid was dried at 60 °C overnight to obtain the final product (0.1 g, 0.2 g, 0.3 g, 0.4 g, respectively, labelled as 1Fe/Mo, 2Fe/Mo, 3Fe/Mo and 4Fe/Mo according to the nanoparticle content). This article focuses on the study of 3Fe/Mo.

Preparation of the working electrode

Typically, 5 mg of catalyst and 40 μL of Nafion solution (5 wt%) were dispersed in 480 μL of ethanol and 480 μL of water by sonication for 1 h to form a uniform black ink. Next, 20 μL of ink was uniformly loaded onto a carbon cloth with an area of (1 × 1 cm) to prepare a working electrode (catalyst loading: 0.1 $mg \cdot cm^{-2}$).

EAS measurements

All electrochemical measurements of EAS were performed in an H-cell system separated by a Nafion 117 membrane. The potential was controlled by an electrochemical workstation (CHI 760E) with a standard three-electrode system. The catalyst was supported on carbon cloth as working electrode, and platinum mesh and saturated Ag/AgCl electrode were used as counter electrode and reference electrode, respectively.

All potentials in this work were converted to reversible hydrogen electrode (RHE) potential as a reference scale by using the Nernst equation (E(vs. RHE) = E(vs. Ag/AgCl) + 0.61 V). EAS was performed in 0.05 M H_2SO_4 solution under mild conditions. Before the EAS test, N_2 gas was purged into the catholyte for 30 min to remove residual air in the H-cell system. During the EAS test, N_2 gas was continuously passed into the cathode chamber for 2 hours at the specified applied potential.

Determination of NH_3

Indophenol blue methods spectrophotometrically: The concentration of generated ammonia was quantitatively determined by the indophenol blue method. Specifically, 2 ml of electrolyte solution was firstly taken from the cathode chamber, and then 2 ml of NaOH (1 M) mixed solution of salicylic acid (5 wt%) and sodium citrate (5 wt%), 1 ml of NaClO solution (0.05 M), 0.2 ml sodium nitroferricyanide ($C_5FeN_6Na_2O \cdot 2H_2O$) solution (1 wt%). After standing for 2 h in a dark light environment at room temperature, the absorbance of the solution at λ = 655 nm was measured with a UV-Vis spectrophotometer. Concentration-absorbance curves were calibrated using standard NH_4Cl solutions at different concentrations (0.1, 0.2, 0.3, 0.4, 0.5 and 0.8 μg/mL) in 0.05 M H_2SO_4. The fitted curve (y = 0.3958 x - 0.00636, R^2 = 0.997) shows a good linear relationship between absorbance values and NH_3 concentration.

Ion chromatography: The electro-reduced ammonia was detected by ion chronograph. In specific, 2 mL postelectrolyzed electrolyte was filtered by a nylon membrane filter (220 nm) and then injected directly into the ion chronograph. The NH_4^+

calibration curves were established by a set of standard solutions with different ammonia sulfide concentrations. The signal of NH_4^+ in ion chronograph spectra was located at 4.2 min.

The NH_3 yield was calculated by the following formula:

$$NH_3 \text{ Yield rate} = (c_{NH3} \times V) / (t \times m)$$

The Faradaic efficiency was calculated as follows:

$$\text{Faradaic efficiency} = (3F \times c_{NH3} \times V) / 17Q$$

where c_{NH3} is the measured NH_3 concentration, V is the volume of electrolyte in the cathode compartment, t is the reduction reaction time (2 h), and m is the catalyst loading on the carbon cloth. F is Faraday's constant (96485 C mol^{-1}) and Q is the total charge passing through the electrode.

$^{15}N_2$ Isotope Labeling Experiments.

After conducting continuous electrolytic tests for a duration of 10 hours utilizing $^{14}N_2$ and $^{15}N_2$ as feeding gas, the electrolyte was obtained. Thereafter, a solution of 25 mL was collected and its pH was adjusted to 3 by adding 2 M HCl. This solution was subsequently concentrated to a volume of 1.5 mL. The resultant liquid was extracted and combined with an internal standard consisting of 0.05 mL of 2 M HCl and 0.08 mL dimethyl sulfoxide (DMSO).

Determination of N_2H_4

The intermediate N_2H_4 during NRR was estimated by the method of Watt and Chrisp,

first, by mixing dimethylaminobenzaldehyde (5.99 g), HCl (30 mL) and C_2H_5OH (300 mL) as a chromogenic reagent. Remove 5 mL of electrolyte and mix with the colour developer (5 mL) prepared above. After stirring at room temperature for 20 minutes, the absorbance of the resulting solution was measured at 455 nm, and the N_2H_4 yield was estimated from a standard curve.

Details of Density Functional Theory (DFT) Calculations

All the density functional theory (DFT) calculations were performed using the Vienna ab-initio simulation package (VASP). The description of the exchange correlation adopted the generalized gradient approximation (GGA) of the Perdew, Burke, and Ernzerhof form. The plane wave energy cutoff was set to 500 eV. The generalized gradient approximation (GGA) with the Perdew-Burke-Ernzerhof (PBE) exchange-correlation functional. The 3 × 3 × 1 monolayer $MoSe_2$ and 2 × 2 ×1 Fe_2O_3 (001) were employed to model the two kinds of samples, while their combination was used to model the $Fe_2O_3/MoSe_2$ interface. In addition, one $MoSe_2$ unit cell and two Se atoms were removed from each 3 × 3 × 1 supercell to build defective $MoSe_2$. The initial spin state of Fe_2O_3 was set to the antiferromagnetic state, and the self-repulsion of the localized d electrons of Fe was taken into consideration within the Hubbard-U scheme (Ueff = 5.3 eV). The energy and force criterion for convergence of the electron density was set at 10-5 eV and 0.03 eV/Å, respectively. The vacuum space along the z-direction was set to 25 Å to avoid interactions between adjacent images.

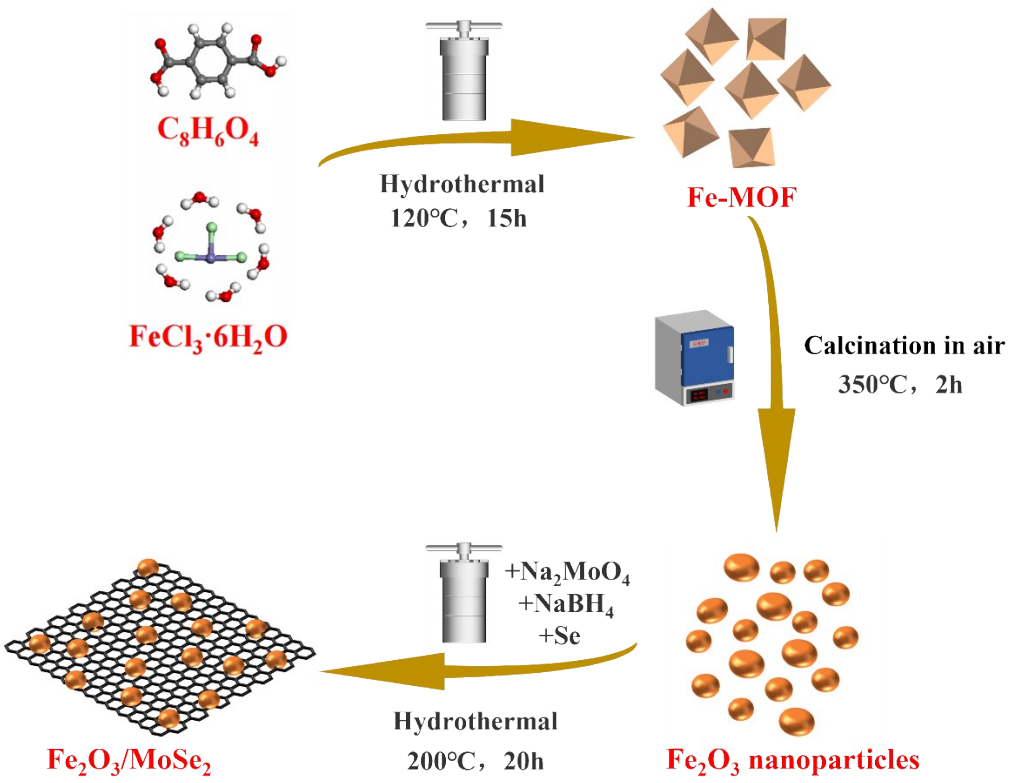

Figure S1. Synthesis process of $Fe_2O_3/MoSe_2$ heterostructure.

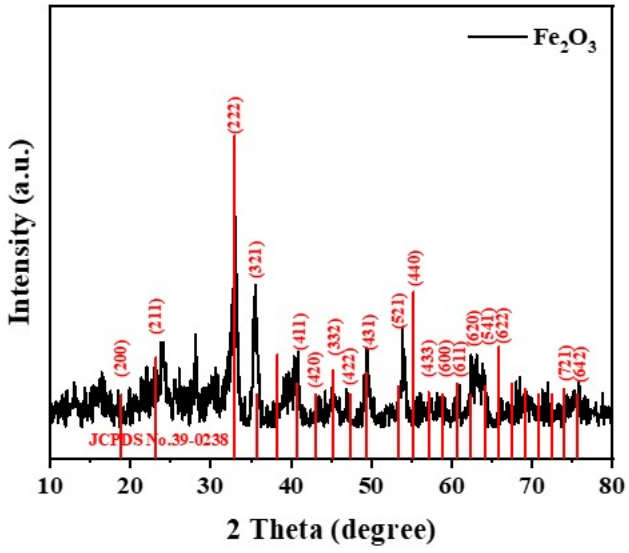

Figure S2. XRD pattern of as-synthesized Fe_2O_3.

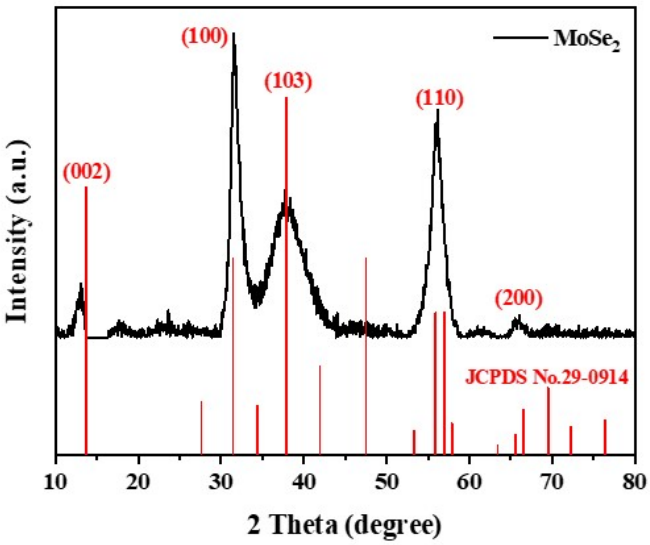

Figure S3. XRD pattern of as-synthesized $MoSe_2$.

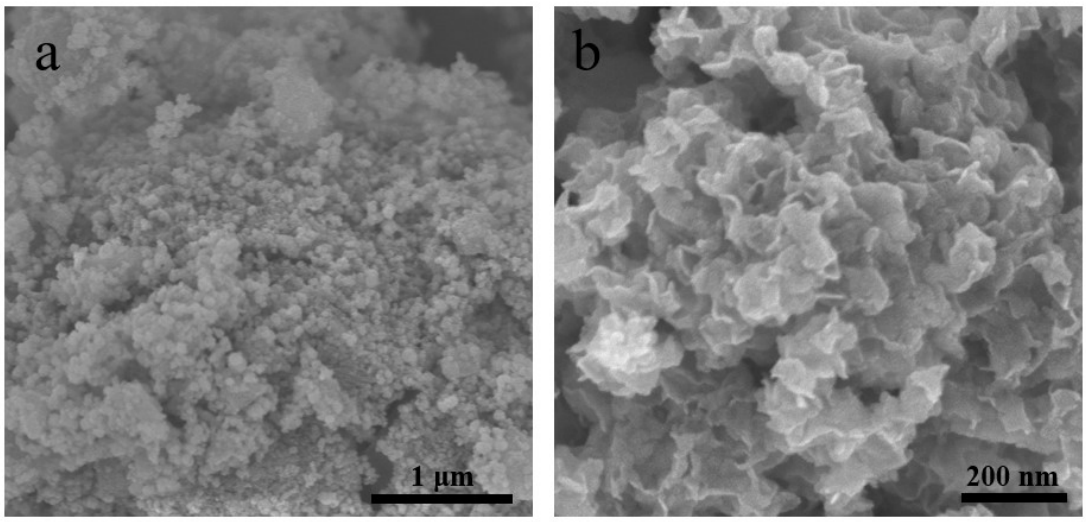

Figure S4. SEM images of (a) Fe_2O_3 and (b) $MoSe_2$.

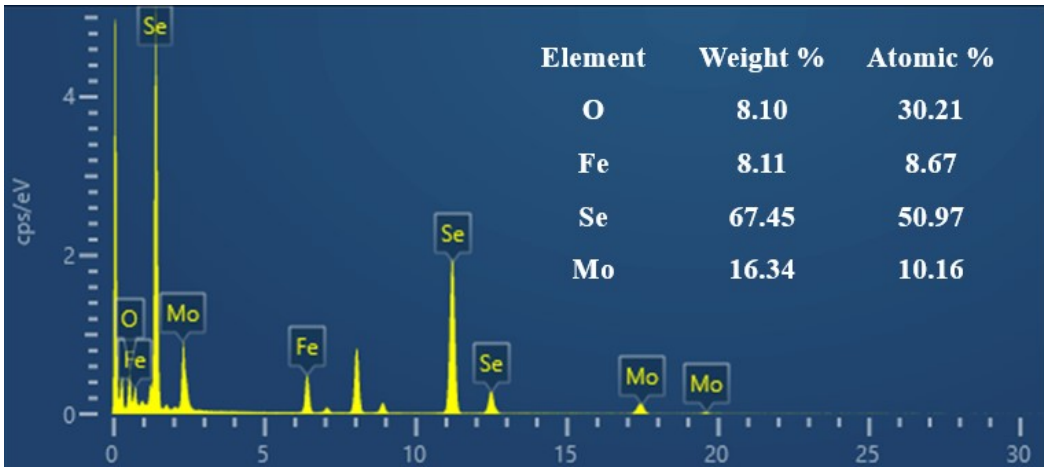

Figure S5. EDX spectra of $Fe_2O_3/MoSe_2$.

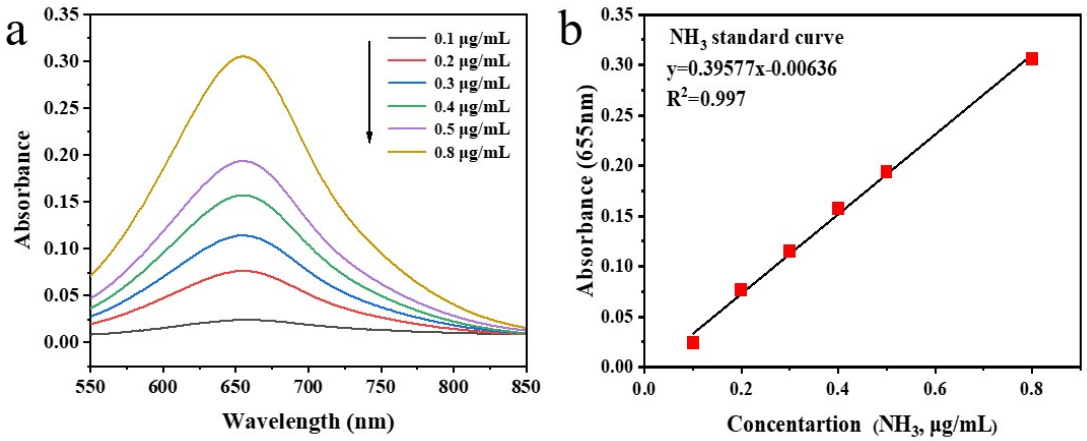

Figure S6. (a) UV-Vis absorption spectra of indophenol assays with NH_4Cl after incubated for 2 h at ambient conditions. (b) Calibration curve used for calculation of NH_3 concentrations.

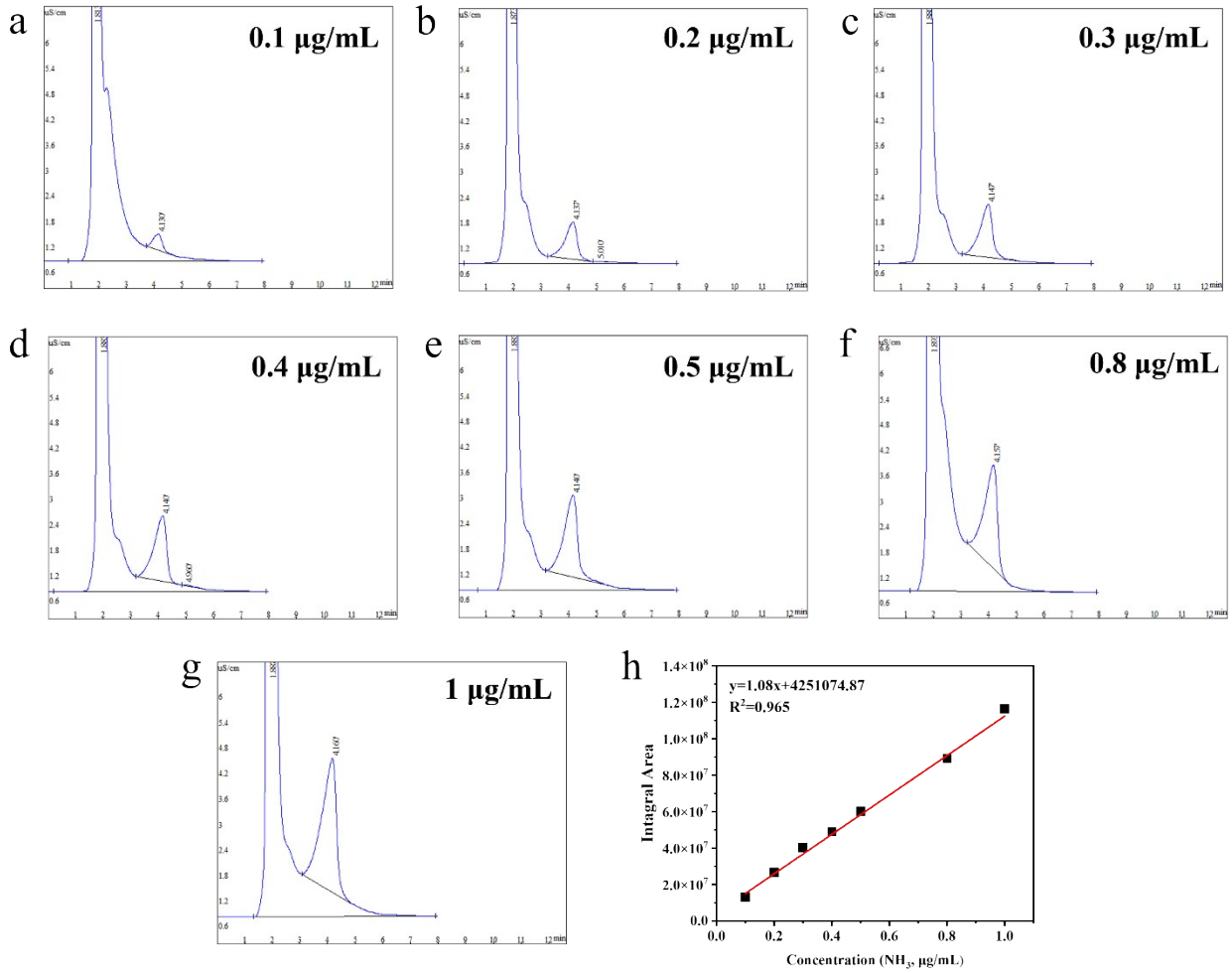

Figure S7. (a-g) Ion chromatography spectra for NH_4^+ions with various concentrations. (h) Calibration curve of NH_4^+.

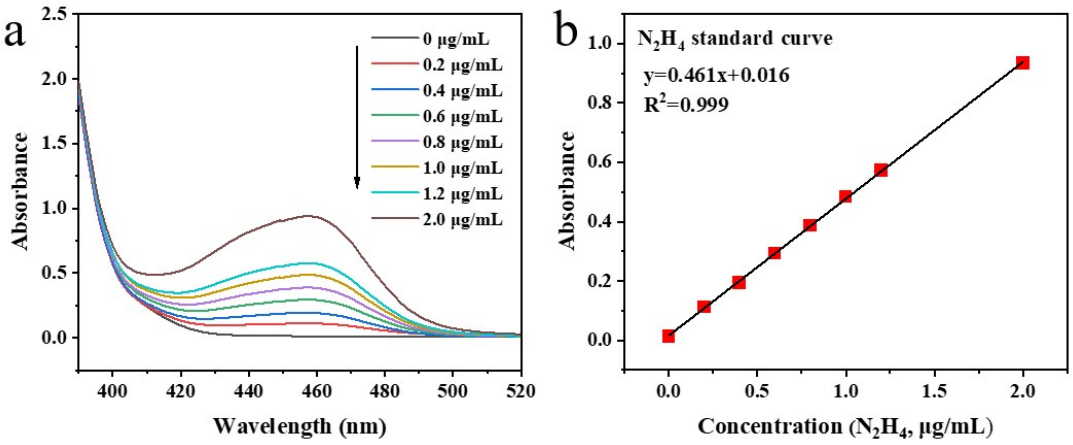

Figure S8. (a) UV-Vis absorption spectra of N_2H_4 assays after incubated for 20 min at ambient conditions. (b) Calibration curve used for calculation of N_2H_4 concentrations.

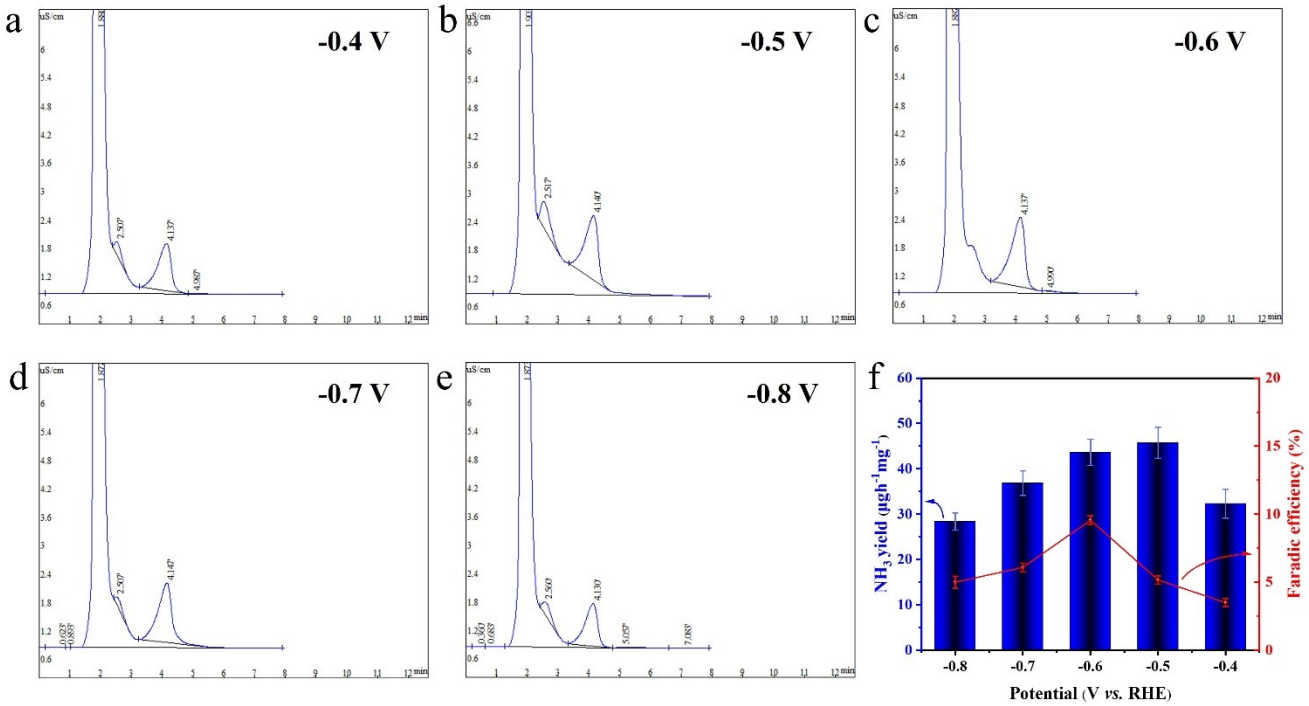

Figure S9. (a-e) Ion chromatography spectra of $Fe_2O_3/MoSe_2$ at various potentials. (f) Calculated NH_3 yield rates and FEs of $Fe_2O_3/MoSe_2$ based on Ion chromatography spectra.

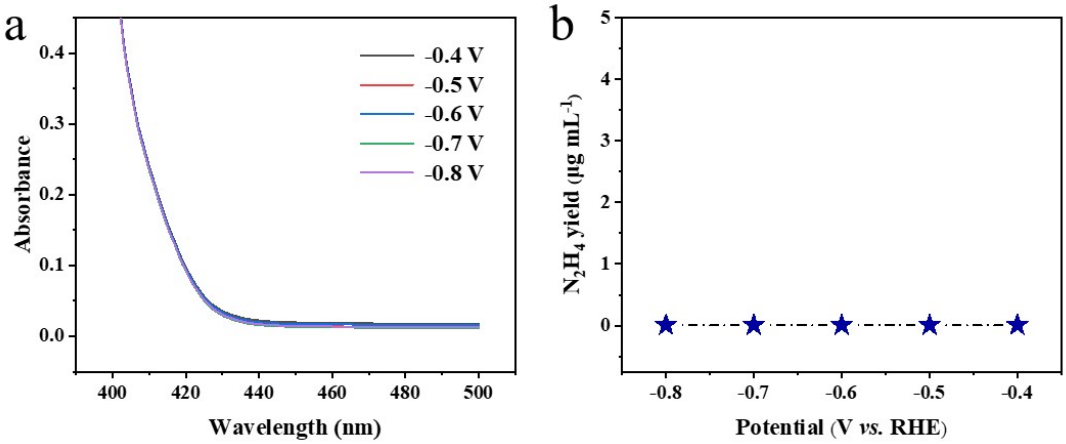

Figure S10. (a) UV-Vis spectra of the electrolytes (stained with the chemical indicator based on the method of Watt and Chrisp) after 2 h electrocatalysis on $Fe_2O_3/MoSe_2$ at various potentials, and (b) corresponding N_2H_4 concentrations in the electrolytes.

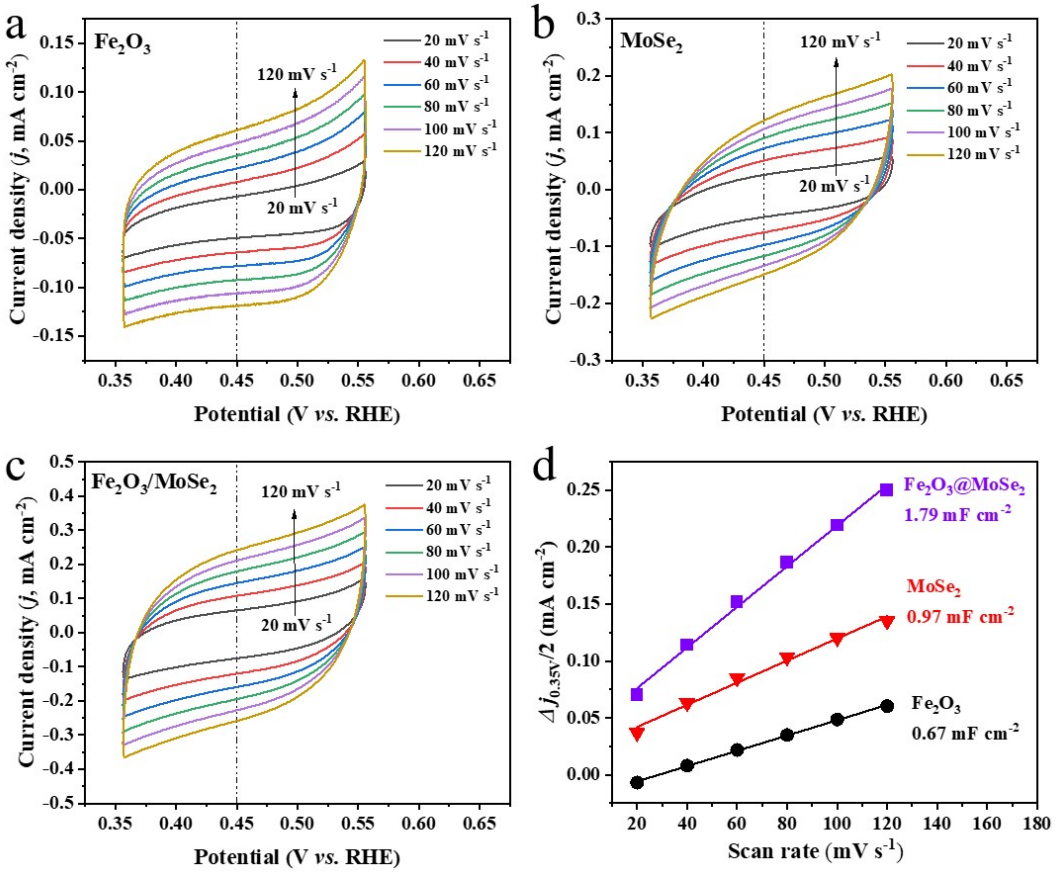

Figure S11. CV curves of (a) Fe_2O_3, (b) $MoSe_2$, and (c) $Fe_2O_3/MoSe_2$ at various scan rates, and corresponding (d) plots of current density differences (Δj/2) vs. scan rate at 0.45 V vs. RHE.

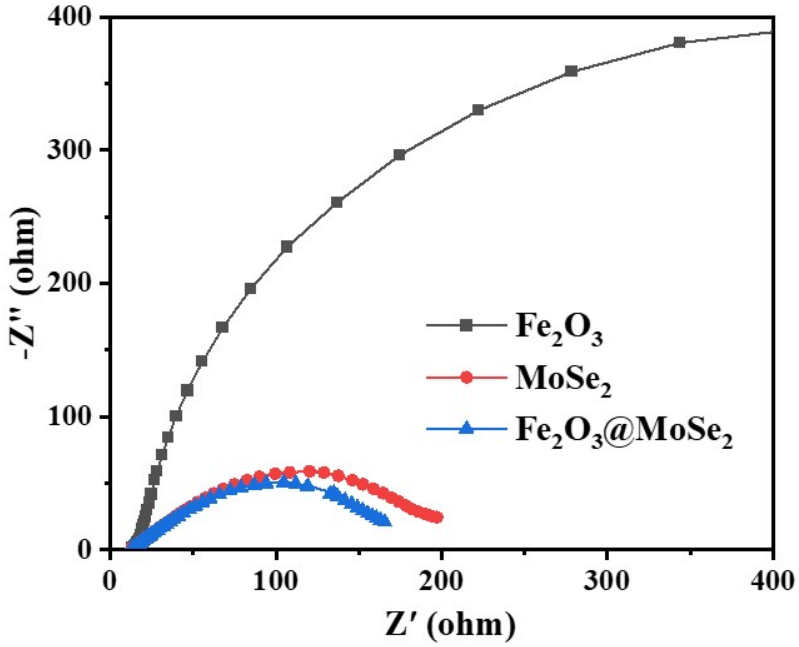

Figure S12. Electrochemical impendence spectra of Fe_2O_3, $MoSe_2$ and $Fe_2O_3/MoSe_2$.

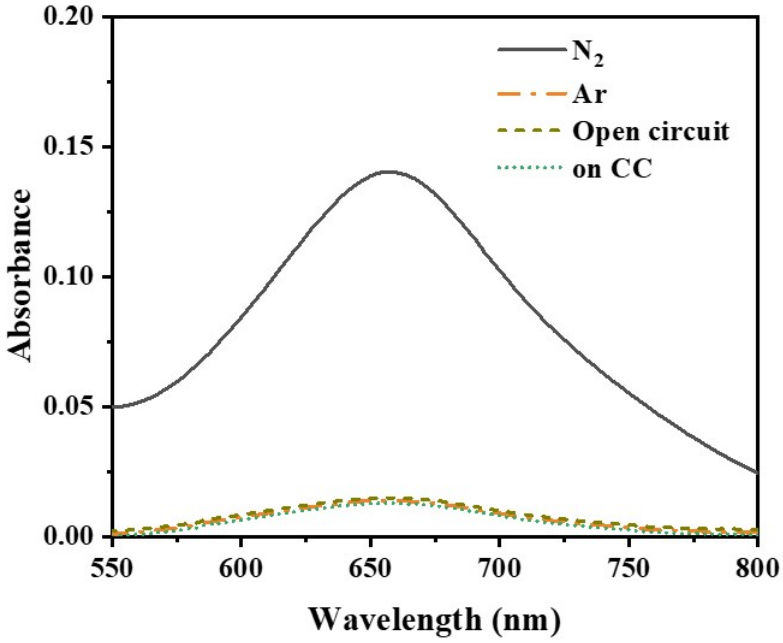

Figure S13. UV-Vis absorption spectra of working electrolytes after 2 h of electrolysis in N_2-saturated solution and Ar-saturated solutions on $Fe_2O_3/MoSe_2$ at -0.5 V, N_2-saturated solution on $Fe_2O_3/MoSe_2$ at open circuit, and N_2-saturated solution on pristine CC at -0.5 V.

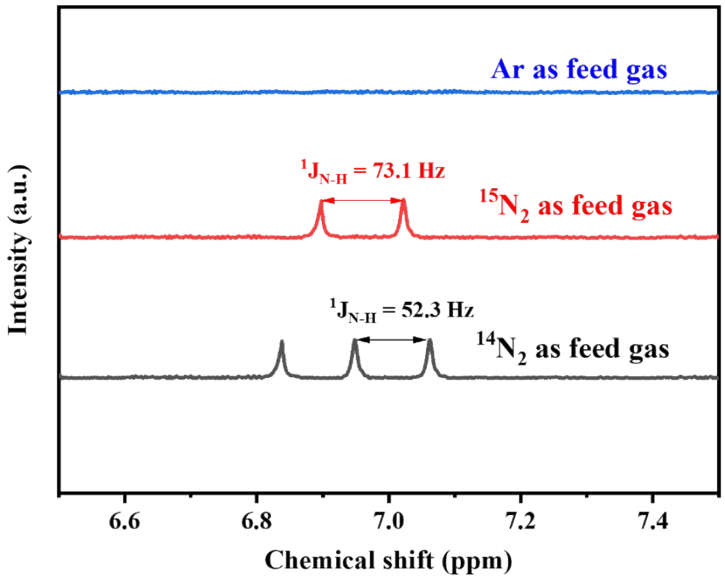

Figure S14. ^{1}H NMR measurements using $^{14}N_2$, $^{15}N_2$ and Ar as feed gases.

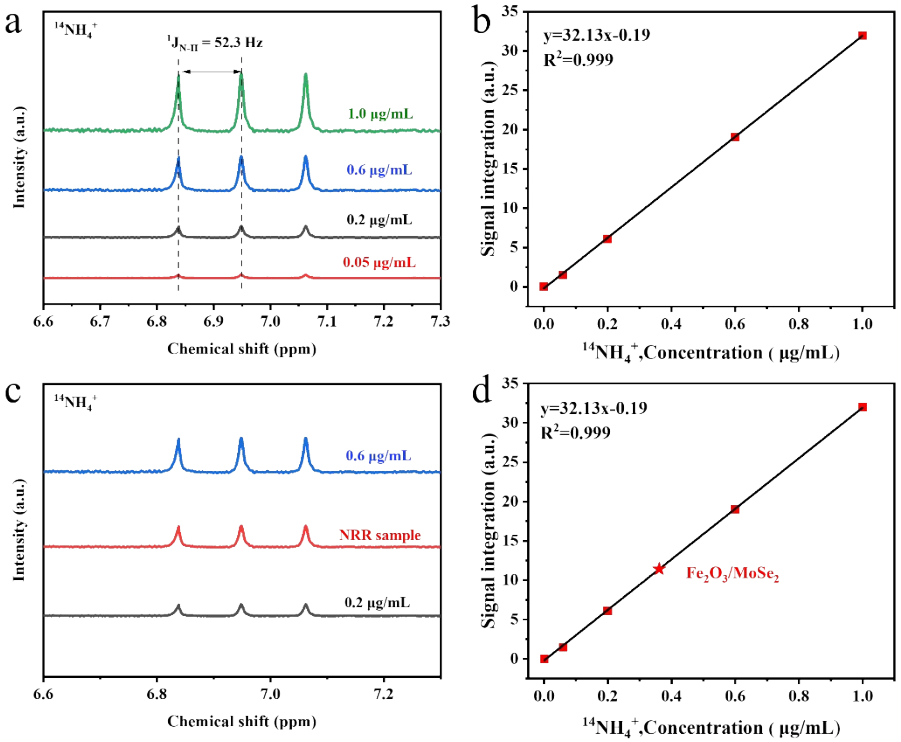

Figure S15. (a) ^{1}H NMR spectra of various concentration of standard $^{14}NH_4$ solution, and (b) its corresponding standard curve. (c) ^{1}H NMR spectra of the electrolyte, and (d) its corresponding concentration of $^{14}NH_4$ electrolysed by $Fe_2O_3/MoSe_2$ at the potential of -0.5 V vs RHE.

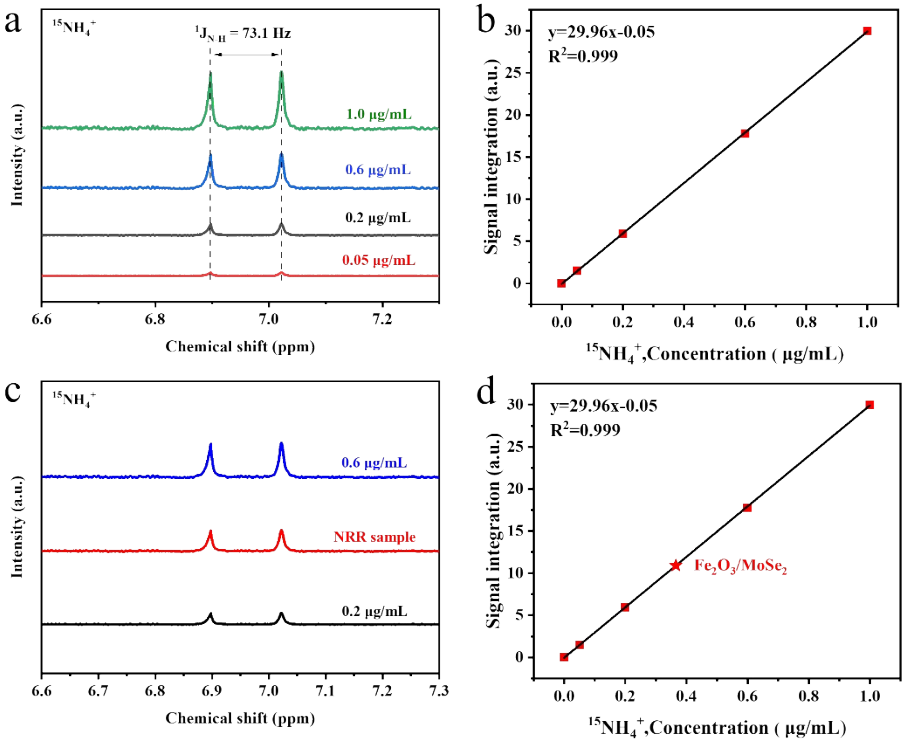

Figure S16. (a) ^{1}H NMR spectra of various concentration of standard $^{15}NH_4$ solution, and (b) its corresponding standard curve. (c) ^{1}H NMR spectra of the electrolyte, and (d) its corresponding concentration of $^{15}NH_4$ electrolysed by $Fe_2O_3/MoSe_2$ at the potential of -0.5 V vs RHE.

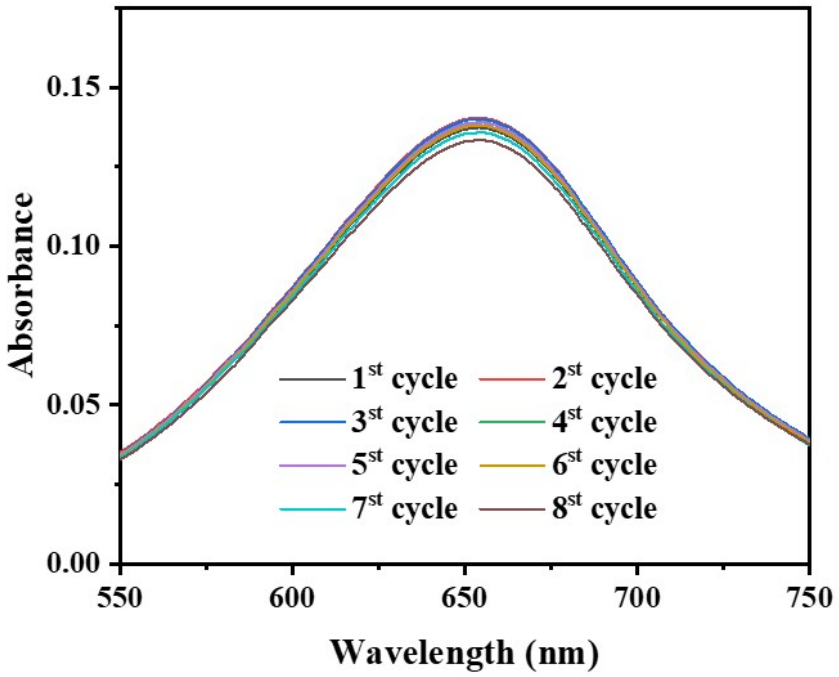

Figure S17. UV-Vis absorption spectra of working electrolytes on $Fe_2O_3/MoSe_2$ (each for 2 h of NRR electrolysis at -0.5 V) for seven cycles.

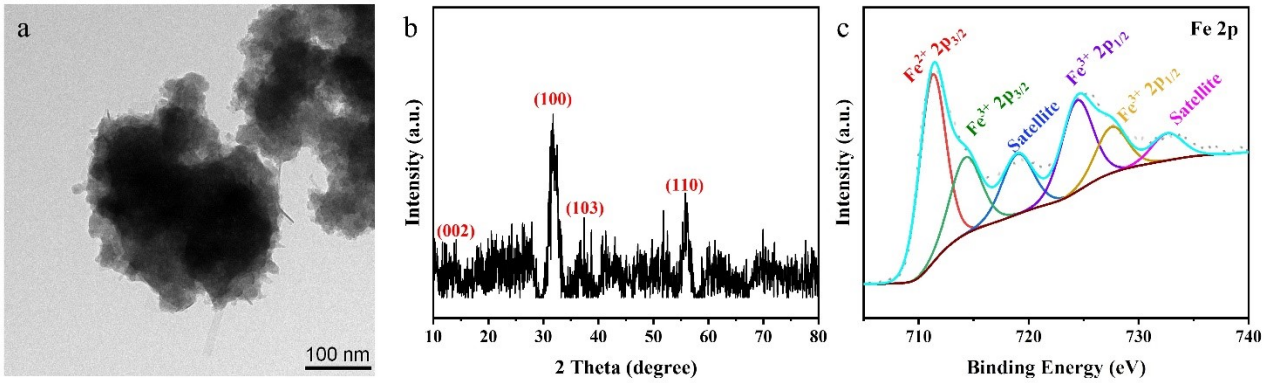

Figure S18. (a) Morphologies, (b) XRD pattern, and (c) XPS survey spectra of $Fe_2O_3/MoSe_2$ after NRR test.

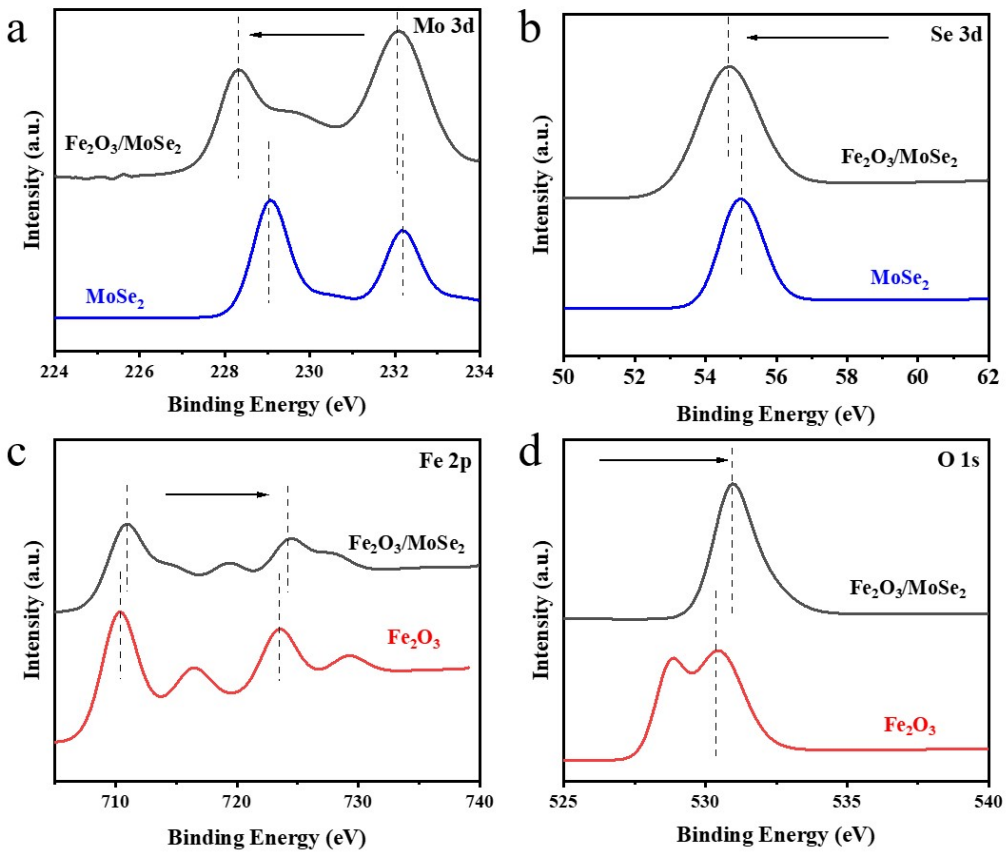

Figure S19. (a, b) High resolution XPS spectra of $MoSe_2$ and $Fe_2O_3/MoSe_2$: (a) Mo 3d, (b) Se 3d. (c, d) High resolution XPS spectra of Fe_2O_3 and $Fe_2O_3/MoSe_2$: (c) Fe 2p, (d) O 1s.

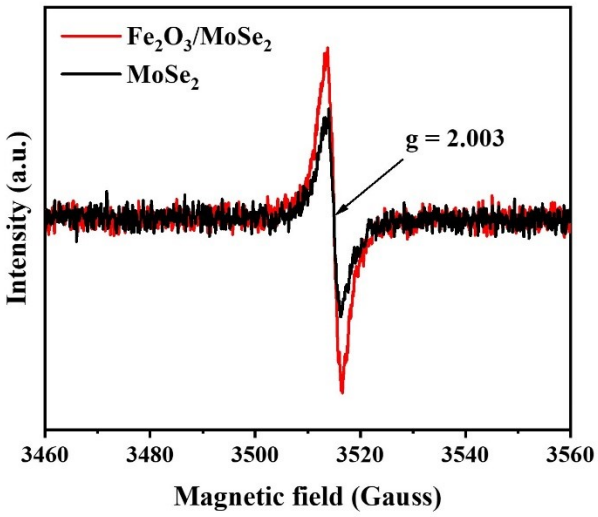

Figure S20. EPR spectra of $MoSe_2$ and $Fe_2O_3/MoSe_2$.

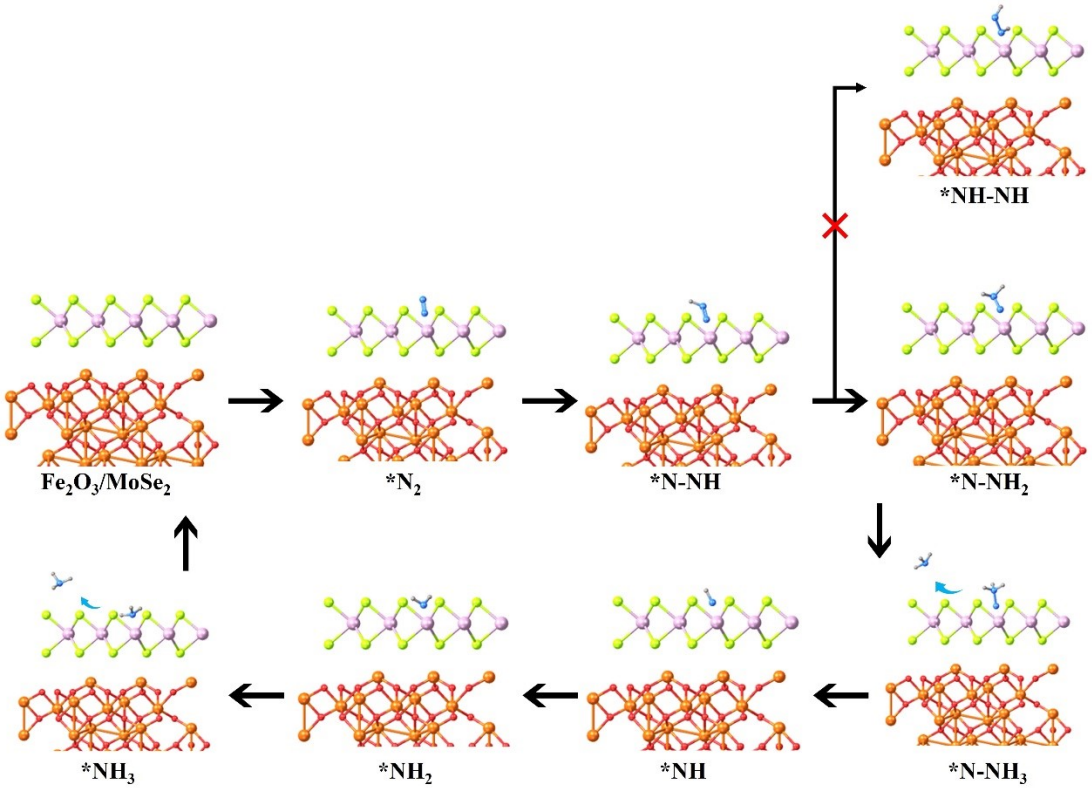

Figure S21. Optimized structures of two reaction pathways. (Color notation: purple-Mo, green-Se, orange-O, red-Fe, blue-N, grey -H).

Table S1. The comparison of $Fe_2O_3/MoSe_2$ catalyst with the representative reported catalysts for electrochemical NRR in aqueous solutions.

Catalyst	Electrolyte	NH_3 yield rate ($\mu g h^{-1} mg_{mat}^{-1}$)	Faraday Efficiency (%)	Ref.
$Fe_2O_3/MoSe_2$	0.05 M H_2SO_4	46.25	9.6	This work
Au_{SA}/np-$MoSe_2$	0.1 M Na_2SO_4	30.83	37.82	[2]
$Fe_2(MoO_4)_3$	0.1 M Na_2SO_4	7.5	1.0	[3]
Vo-MoO_2/C	0.1M Na_2SO_4	9.75	3.24	[4]
$Cu_{2-x}S/MoS_2$	0.1 M HCl	22.1	6.06	[5]
$FeMoO_4$	0.1M Na_2SO_4	17.51	10.5	[6]
Fe SAs/MoS_2	0.1 M K_2SO_4	8.63	18.8	[7]
Au-Fe_3O_4	0.1 M KOH	21.42	10.54	[8]
1T′-MoS_2/Ti_3C_2	0.1 M Na_2SO_4	31.96	30.75	[9]
Nb_2O_5/C-800	0.1 M HCl	29.1	11.5	[10]
MoS_2/rGO	0.5 M Li_2ClO_4	24.82	4.58	[11]
$V_4C_3T_x$	0.1 M KOH	21.29	8.04	[12]
CoS/S-MAs ($Ti_3C_2T_x$ MXene)	0.1 M Na_2SO_4	12.4	27.05	[13]
Ru SAs/Ti_3C_2O	0.1 M HCl	27.56	23.3	[14]

References

1. P. Man, Q. Zhang, Z. Zhou, M. Chen, J. Yang, Z. Wang, Z. Wang, B. He, Q. Li and W. Gong, *Advanced Functional Materials*, 2020, **30**, 2003967.
2. D. Chen, M. Luo, S. Ning, J. Lan, W. Peng, Y. R. Lu, T. S. Chan and Y. Tan, *Small*, 2022, **18**, 2104043.
3. C. Chen, Y. Liu and Y. Yao, *European Journal of Inorganic Chemistry*, 2020, **2020**, 3236-3241.
4. Y. Du, Z. He, F. Ma, Y. Jiang, J. Wan, G. Wu and Y. Liu, *Inorganic Chemistry*, 2021, **60**, 4116-4123.
5. T. Jiang, L. Li, L. Li, Y. Liu, D. Zhang, D. Zhang, H. Li, B. Mao and W. Shi, *Chemical Engineering Journal*, 2021, **426**, 130650.
6. J. Wu, Z. Wang, S. Li, S. Niu, Y. Zhang, J. Hu, J. Zhao and P. Xu, *Chemical Communications*, 2020, **56**, 6834-6837.
7. H. Su, L. Chen, Y. Chen, R. Si, Y. Wu, X. Wu, Z. Geng, W. Zhang and J. Zeng, *Angewandte Chemie*, 2020, **132**, 20591-20596.
8. J. Zhang, Y. Ji, P. Wang, Q. Shao, Y. Li and X. Huang, *Advanced Functional Materials*, 2020, **30**, 1906579.
9. X. Chen, S. Zhang, X. Qian, Z. Liang, Y. Xue, X. Zhang, J. Tian, Y. Han and M. Shao, *Applied Catalysis B: Environmental*, 2022, **310**, 121277.
10. M. Zhang, H. Yin, F. Jin, J. Liu, X. Ji, A. Du, W. Yang and Z. Liu, *Green Energy & Environment*, 2022.
11. Y. Li, J. Li, J. Huang, J. Chen, Y. Kong, B. Yang, Z. Li, L. Lei, G. Chai and Z. Wen, *Angewandte Chemie*, 2021, **133**, 9160-9167.
12. C.-F. Du, L. Yang, K. Tang, W. Fang, X. Zhao, Q. Liang, X. Liu, H. Yu, W. Qi and Q. Yan, *Materials Chemistry Frontiers*, 2021, **5**, 2338-2346.
13. Q. Li, T. Song, Z. Wang, X. Wang, X. Zhou, Q. Wang and Y. Yang, *Small*, 2021, **17**, 2103305.
14. G. Chen, M. Ding, K. Zhang, Z. Shen, Y. Wang, J. Ma, A. Wang, Y. Li and H. Xu, *ChemSusChem*, 2022, **15**, e202102352.